Protolytic Photodissociation and Proton-Induced Quenching of 1-Naphthol and 2-Octadecyl-1-Naphthol in Micelles

Kyril M. Solntsev,*,† Sami Abou Al-Ainain,‡ Yuri V. Il'ichev,§ and Michael G. Kuzmin

Department of Chemistry, Moscow State University, Moscow, 117234, Russia

Received: March 8, 2004; In Final Form: July 14, 2004

Kinetics of excited-state proton-transfer reactions and proton-induced fluorescence quenching of 1-naphthol (1N) and 2-octadecyl-1-naphthol (2O1N) in micellar solutions of cetyltrimethylammonium bromide (CTAB), polyoxyethylene(23) lauryl ether (Brij 35), and sodium dodecyl sulfate (SDS) was studied by using stationary and time-resolved fluorescence techniques. The ground-state acidity constant of 2O1N in cationic micelles of CTAB was found to be significantly smaller than that of the parent compound ($\Delta pK = 0.5$). However, similar rate and equilibrium constants of the protolytic dissociation were obtained for 1N and 2O1N in the singlet excited state. Effects of nonionic micelles of Brij 35 closely resemble those of CTAB. In anionic micelles of SDS, the protolytic photodissociation was much slower for 2O1N than for 1N. The protonation rate for the excited anions in micellar solutions increases by approximately 2 orders of magnitude in the series CTAB, Brij 35, SDS. Excited-state kinetics was rationalized within the framework of a pseudophase model, which included micellar effects on the proton-transfer equilibrium and interfacial diffusion of hydronium ions. The electrostatic surface potential of charged micelles was estimated from the acidity constants of naphthols.

Introduction

Proton transport in proteins and lipid bilayers is of paramount importance for bioenergetics.[1−5] This stimulates high research activity in the field of proton-transfer dynamics in organized molecular systems.[6−12] Aromatic photoacids and bases have found use as proton-transfer fluorescent probes for surfactant assemblies and macromolecules.[7,13−15] Such probes have been utilized by our group[16−22] and some other workers[7,15,23−29] to elucidate effects of the microenvironment on the equilibrium and rate constants of the excited-state proton transfer in micelles, liposomes, microemulsions, and LB films. Effects of the surface potential on apparent pK[15] and protolytic photodissociation rate constants,[22] correlation between rate constants and apparent pK in micelles of different charge,[16,21] and kinetic nonequivalence of proton-transfer probes in liposomes[18] have been revealed. However, advantages of proton-transfer fluorescent probes are still not fully recognized and utilized in studies of molecular organized systems, although other spectroscopic probes enjoy very wide applications in such studies.[14,15,30−32]

Recently, we have introduced several long-chain alkyl derivatives of naphthols[20,21] as promising fluorescent probes for complex microenvironments of surfactant assemblies and biological macromolecules. Both hydrophobic naphthols and their anions are expected to be completely solubilized in the organic microphase, i.e., the interfacial exchange is much slower than the fluorescence decay. Various derivatives may differ in a reactive-group localization site depending on the size and relative position of an alkyl substituent. In our previous study,[21] kinetics of the photodissociation of 2-naphthol (2N) and its long-chain alkyl derivatives have been characterized. Unfortunately, this study was limited to cationic micelles because of slow photodissociation of 2N derivatives in other surfactant assemblies. Here, we report kinetic data for much stronger photoacids, 2-octadecyl-1-naphthol (2O1N) and 1-naphthol (1N), in positively charged (cetyltrimethylammonium bromide, CTAB), negatively charged (sodium dodecyl sulfate, SDS), and uncharged micelles (Brij-35). Results of a comparative study of 2O1N and 1N in homogeneous solutions will be described elsewhere.[33] 1-Naphthol derivatives provide an opportunity to probe protolytic reactions in a variety of microheterogeneous systems as well as in mixed homogeneous solutions. Pronounced photodissociation of 1N has been observed in micelles of anionic and nonionic surfactants, in lipid bilayers, and in negatively charged microemulsions.[15,18,22,27−29]

SCHEME 1

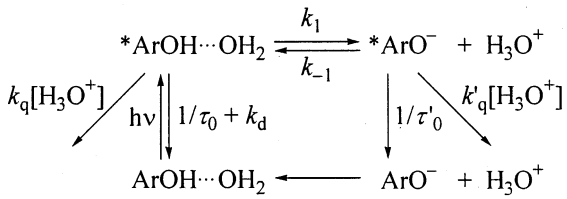

Analysis of the photodissociation kinetics for 1-naphthol derivatives is complicated by efficient proton-induced fluorescence quenching.[33,34] Nevertheless, apparent rate constants and even kinetic parameters for elementary reactions can be evaluated by using a simple scheme including proton-induced radiationless deactivation (see Scheme 1, where k_1 and k_{-1} are apparent rate constants of excited-state protolytic dissociation and back adiabatic protonation, τ_0 and τ'_0 are the lifetimes of *ArOH and *ArO$^-$ in the absence of the protolytic reactions, k_q and k_q' refer to the apparent rate constants of *ArOH and

* To whom correspondence should be addressed: School of Chemistry and Biochemistry, Georgia Institute of Technology, Atlanta, GA 30332-0400, USA. Phone: (404)385-1384. Fax: (404) 894-7452. E-mail: solntsev@chemistry.gatech.edu.

† Present address: School of Chemistry and Biochemistry, Georgia Institute of Technology, Atlanta, GA 30332-0400, USA.

‡ Permanent address: Department of Chemistry, Faculty of Science, Tishreen University, Latakia, Syria.

§ Present address: Department of Chemistry, Wichita State University, Wichita, KS 67260, USA.

10.1021/jp040201f CCC: $27.50
Published on Web 09/10/2004

*ArO^- quenching by hydronium ions, and k_d is the apparent rate constant of radiationless deactivation competing with the adiabatic dissociation). Kinetics of proton-transfer reactions in micelles and the majority of effects observed have been rationalized within the framework of a similar kinetic scheme and a pseudo phase model of surfactant assemblies.[15−20] The model treats surfactant aggregates as a "pseudophase" having properties different from the bulk aqueous phase.[35−37] The model ignores complex internal structure of micelles and assumes that all probe molecules located in the micellar pseudophase have identical properties due to fast intramicellar averaging. The pseudophase model also implies fast (relative to fluorescence lifetimes) exchange of hydronium and hydroxyl ions between the micellar and bulk phases and operates with apparent acidity and rate constants. These apparent constants depend on the activities of hydronium ions in the micellar and aqueous phases and, therefore, on the charge and microscopic polarity of micelles. Such a formal treatment has advantages and disadvantages similar to those of the use of formal p*K* and pH scales in nonaqueous systems. But two important merits of this approach are evident: possibilities to consider the passive and active proton transport in complex organized molecular systems in terms of local electrochemical potentials[15,38] and to use empirical relationships to reveal actual mechanisms and laws governing proton transport in organized molecular systems.

Experimental Section

1N (Merck) was purified by vacuum sublimation. 2O1N was synthesized according to slightly modified procedures from literature.[39] A mixture of 1N and stearic acid with a molar ratio of 1.25 was heated in CCl_4 for 2 h. Gaseous BF_3 was constantly bubbled through the solution. 2-Octadecanoyl-1-naphthol obtained was recrystallized several times from ethanol (melting point T_m = 86 °C). A toluene solution of 2-octadecanoyl-1-naphthol was mixed with aqueous HCl containing freshly prepared Zn/Hg. The mixture was bubbled with gaseous HCl and heated for ca. 30 h. 2O1N (T_m = 62 °C) was purified by column chromatography on silica gel (Chemapol) with toluene as an eluent. Thin-layer chromatography on silica gel (Kavalier) with the same solvent gave an R_f value of 0.4. ^{1}H NMR (300 MHz, $CDCl_3$, room temperature, *J*/Hz): δ = 8.18 (dd, 1H, 8 arom., J = 5.8 and 2.8); 7.76 (dd, 1H, 5 arom., J = 5.6 and 2.4); 7.36−7.51 (m, 2H, 6 and 7 arom.); 7.38 (d, 1H, 3 arom., J = 8.0); 7.23 (d, 1H, 4 arom., J = 8.0); 5.14 (s, 1H, **H**O-group); 2.75 (t, 2H, C**H$_2$**−Ar, J = 7.8); 1.72 (m, 2H, −C**H$_2$**−CH_2Ar), 1.12−1.52 with a maximum at 1.33 (m, 30H, methylene chain); 0.86 (t, 3H, C**H$_3$**, J = 6.0 and 6.9).

CTAB (Sigma), polyoxyethylene(23) lauryl ether, Brij 35 (Merck), and SDS (Aldrich) were free from fluorescent impurities and used as received. HCl and NaOH were of analytical grade. Deionized water was used in all experiments. Sodium chloride was recrystallized from water. All experiments were performed at room temperature (21−22 °C), except for measurements in CTAB micellar solutions, which were done at 40 °C. The micellar solutions containing naphthols were prepared as follows: a surfactant and naphthol were initially dissolved in absolute ethanol, solvent was removed in a vacuum, and the residual was dissolved in hot water. The surfactant concentrations were kept constant and equal to 50, 10, and 100 mM for CTAB, Brij 35, and SDS solutions, respectively. These concentrations were well above critical micellar concentrations. Concentrations of 1N and 2O1N did not exceed 0.1 mM. At pH < 7, 1N was almost completely solubilized (>99%) in the micellar phase formed by various surfactants under experimental conditions used in this work.[16−18] To avoid variations in the micellar surface potential and the hydronium ion activity with electrolyte concentration,[14,15] all experiments in micellar solutions were performed at a constant ionic strength of 250 mM stabilized by adding NaCl.

pH values were measured with an ionometer I-120 (Russia) equipped with a glass electrode calibrated with standard aqueous buffers. ^{1}H NMR spectra were measured with a Bruker AC-200P spectrometer. Absorption spectra were recorded with a Specord M-40 (Carl Zeiss Jena) or a Shimadzu UVPC-2101 spectrophotometer. Fluorescence spectra were measured with a Perkin-Elmer LS-50 luminescent spectrometer. In all cases, relative fluorescence intensities were used instead of quantum yields since no change in the spectral shape was observed at all experimental conditions. The ArO^- fluorescence intensity corresponding to φ_0' (see below) was measured at pH > 12. Isosbestic points with the longest wavelength were selected for excitation in order to calculate the fluorescence quantum yield ratio directly from the intensity ratio. Their values were 315 and 316 nm in CTAB and 308 and 313 nm in Brij 35 micelles for 1N and 2O1N, respectively. For SDS micelles, deprotonation in the ground state is associated with a change in the localization of naphthols, and therefore, the *ArO^- fluorescence quantum yields in the absence of the protolytic reactions cannot be measured correctly (see text). Excitation wavelengths of 306 and 317 nm were selected for 1N and 2O1N, respectively. The *ArO^- fluorescence intensity (I') was corrected for the overlap of *ArOH and *ArO^- fluorescence spectra

$$I' = I_{exp}' - I_{exp}\,(i_0'/i_0) \qquad (1)$$

where I_{exp}' and I_{exp} are the experimental values of the fluorescence intensities at the *ArO^- and *ArOH emission maxima and i_0' and i_0 are the *ArOH fluorescence intensities measured at the same wavelengths as I_{exp}' and I_{exp}, respectively. The corresponding intensities in the emission spectra of the protonated forms of 1N and 2O1N in hexanol or ethanol (no excited-state protolytic dissociation occurred in these solvents) were used to correct the anion spectra according to eq 1.

Fluorescence decay curves were measured with a time-correlated single-photon counting technique. A homemade instrument with an air-flash lamp (full width at half maximum ≈ 1 ns) and ORTEC electronics was used. The excitation wavelength of 313 nm was selected with an interference filter. Decay curves were analyzed by using a nonlinear least-squares iterative deconvolution procedure. All the rate constants were determined from time-resolved and steady-state data by using the same approach as that developed for the reactions in homogeneous solutions (see ref 33 and Appendix).

Results

Cationic Micelles of CTAB. In a 1N solution containing 50 mM CTAB (pH ≈ 6, 40 °C), weak but distinct fluorescence of ArOH (λ_{fl} = 362 nm, Figure 1a) was observed. The *ArO^--to-*ArOH emission intensity ratio (I_N'/I_N) in this solution was much smaller than that in bulk water (see Table 1). This suggested a decrease in the photodissociation rate constant in CTAB micelles. Increasing the HCl concentration in this solution resulted in the quenching of the *ArO^- emission (λ_{fl} = 453 nm), but the *ArOH fluorescence was only slightly enhanced. Figure 1b shows the fluorescence spectra of 2O1N in CTAB micelles measured under the same experimental conditions as those for 1N. At neutral pH, the I_N'/I_N ratio was slightly smaller for 2O1N than for 1N. This might be attributed to a decrease

TABLE 1: Kinetic Parameters of Protolytic Photoreactions of 1N and 2O1N in Micellar Solutions[a]

	CTAB		Brij 35		SDS	
compound	1N	2O1N	1N	2O1N	1N	2O1N
I_N'/I_N	13.6	8.35	1.52	1.03	0.31	0.05
φ_N'/φ_0'	0.80	0.65		0.34		
τ_N/ns	0.68	0.82	2.1	1.6	2.5	2.6
τ_N'/ns	18.7	21.2	15.2	13.9	9.7	6.3
τ_0'/ns	18.9	21.6	15.4[b]	14.3		
pK	9.5	10.0	10.1	11.6	10.5	>13
k_1/ns^{-1}	1.2[c], 2.2[d]	0.81[c], 1.2[d]	0.3[d]	0.22[c], 0.22[d]	0.09[d]	0.02[d]
η	0.9[c], 1.7[d]	0.8[c], 1.1[d]	1.1[d]	0.5[c,d]	0.5[d]	0.1[d]
$(k_{-1} + k_q')$/M^{-1} ns^{-1}	0.65	0.43	7.0	8.8	19	19
k_{-1}/M^{-1} ns^{-1}	0.22[e], 0.40[f], 0.35[g]	0.16[e], 0.21[g]	3.9[e], 5.2[f]	3.5[e], 1.4[g]	18[f]	<19
k_q'/M^{-1} ns^{-1}	0.43[e], 0.25[f], 0.30[g]	0.27[e], 0.22[g]	3.1[e], 1.8[f]	5.4[e], 7.4[g]	1[f]	<19
η'	0.3[e], 0.6[f], 0.5[g]	0.4[e], 0.5[g]	0.6[e], 0.8[f]	0.4[e], 0.2[g]	0.9[f]	
pK*	(−0.5) − (−1)	(−0.6) − (−0.7)	1.1−1.2	0.8−1.2	2.3	∼3
k_q/M^{-1} ns^{-1}	≪0.1[e,f]	≪0.1[e]	0.7[e], 0.5[f]	1[e]	18[e], 20[f]	11[e]
k_{NR}/k_{OUT}	<0.1	<0.3	≪0.1	1	1	7
k_{NR}/k_{-R}	0.6−1.9	1.0−1.7	0.3−0.8	1.5−5.3	0.1	0.1
k_{-R}/k_{OUT}	<0.1	<0.3	<0.1	0.2−0.6	20	90
k_R/ns^{-1}	1−3	1−2	0.3	1	2−8	12
k_{IN}/M^{-1} ns^{-1}	3−5	1−2		12	20−40	

[a] Uncertainties in the decay times were about 10%. [b] Biexponential fluorescence decay was observed; the second decay time was 6.7 ns. [c] $k_1 = \varphi_N'/\varphi_0')(\tau_0'/\tau_N')/\tau_N$, eq A13. [d] $k_1 = [(\varphi_N'/\varphi_N)/(\varphi_0'/\varphi_0)_S](\tau_0'/\tau_0)_S/\tau_N'$, eq A14; $(\varphi_N'/\varphi_N) = I_N'/I_N$; $(\varphi_0'/\varphi_0)_S = (I_0'/I_0)_S = 0.64$ and 0.54 and $(\tau_0'/\tau_0)_S = 1.9$ and 1.6 for 1N and 2O1N, respectively, in absolute ethanol. [e] k_{-1} and k_q from slopes and intercepts of the plots of φ_N/φ against $(\varphi_N\varphi')/(\varphi\varphi'_N)$, eq A10. [f] From time-resolved fluorescence data (see eqs A3−A7) and k_1 values. [g] k_{-1} and k'_q from slopes of the plots in the coordinates corresponding to eqs A11 and A12.

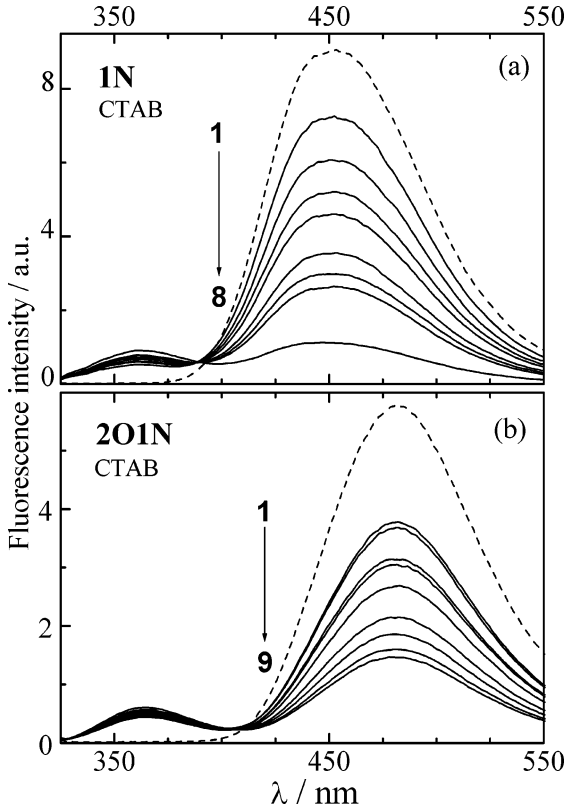

Figure 1. Fluorescence spectra of 1N (a) and 2O1N (b) in 0.05 M CTAB micellar solutions in the presence of ∼0.001 M NaOH (dashed line) or HCl (solid lines). Arrows with numbers refer to *ArO$^-$ fluorescence and represent an increase in HCl concentration, which was 0 (1), 25 (2), 50 (3), 92 (4), 150 (5), 200 (6), 250 (7), and 500 mM (8) for 1N and 0 (1), 6.2 (2), 12.5 (3), 25 (4), 50 (5), 100 (6), 150 (7), 200 (8), 250 mM (9) for 2O1N.

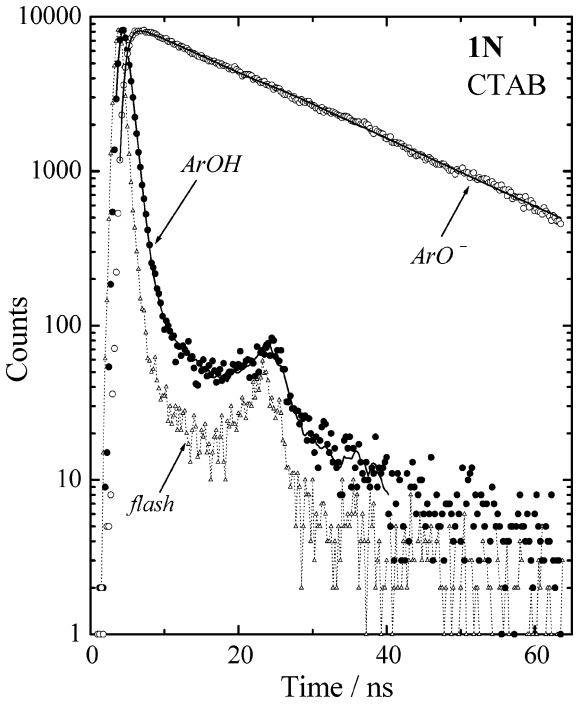

Figure 2. Fluorescence decay curves of neutral (*ArOH) and anionic species (*ArO$^-$) of 1N in 50 mM CTAB micellar solution at pH ≈ 6. The solid lines are the best fits to the data convoluted with the instrument response function labeled as "flash" (dotted line with symbols).

in the photodissociation rate caused by the alkyl substituent. Addition of HCl to the micellar solution affected the 2O1N fluorescence spectra in a similar manner as it did for the parent compound; the *ArO$^-$ fluorescence (λ_{fl} = 483 nm) was quenched, and *ArOH emission (λ_{fl} = 364 nm) intensity was changed very little.

Figure 2 shows fluorescence response functions for neutral and anionic species of 1N in the CTAB solution at neutral pH. The *ArOH fluorescence decay was practically single exponential with a lifetime (τ_N) of 0.68 ns (A < 0.01, see eqs A1 and A4). Fluorescence kinetics for *ArO$^-$ in the same solution was well described by a two-exponential function (eq A2) with a rise time, τ_1, similar to the *ArOH decay time and a decay time $\tau_2 = \tau_N'$ = 18.7 ns. These data confirmed validity of

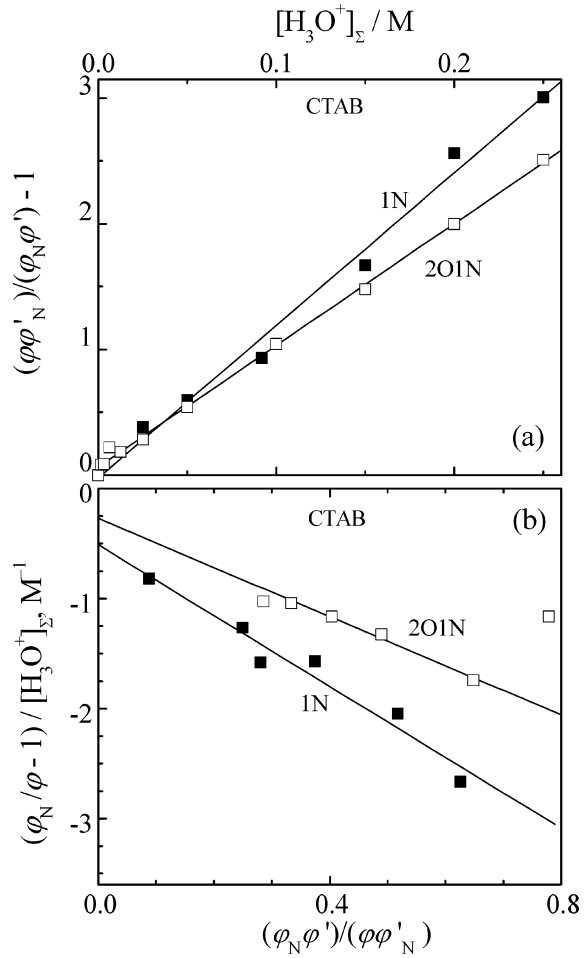

Figure 3. Plots of $(\varphi\varphi_N')/(\varphi_N\varphi') - 1$ vs $[H_3O^+]_\Sigma$ (a) and $(\varphi_N/\varphi - 1)/[H_3O^+]_\Sigma$ vs $(\varphi_N\varphi')/(\varphi\varphi_N')$ (b) for 1N (filled symbols) and 2O1N (open symbols) in 50 mM CTAB micellar solution.

Scheme 1 for 1N in CTAB micellar solutions. Fluorescent lifetimes of 1N in micellar solutions (see Table 1) that were obtained in this work are in agreement with those reported for similar systems by Mandal et al.[29] It is important to note that $*ArO^-$ fluorescence decay was found to be single exponential and $*ArO^-$ fluorescence maximum to be the same for all pH values studied. The fluorescence lifetime and emission maximum of the 1-naphtholate anion are known to be sensitive to its microenvironment.[18,29,40] A longer lifetime in CTAB solutions ($\tau_0' = 18.9$ ns for 1N) as compared to bulk water (8.0 ns) and a large blue shift of the $*ArO^-$ fluorescence maximum in CTAB micelles relative to water, ethanol, and aqueous acetonitrile[33] indicated that the 1N anion was localized in a less polar environment. Therefore, the protolytic photodissociation of 1N took place in the micellar phase and the excited anion remained bound to positively charged micelles. Similar behavior was expected for strongly hydrophobic 2O1N. Parameters of 2O1N fluorescence decay curves in neutral and basic CTAB solutions are presented in Table 1. Very long fluorescence lifetimes of 1N and 2O1N naphtholates determined from purely exponential decay curves exclude slow solvation of these fluorophores in micelles. So, we do not think that the slow transient effects are responsible for a hypsochromic shift of the anion fluorescence spectra. Most probably the latter is due to static solvation effects (lower polarity, etc.). It is noteworthy that the fluorescence decay time of 2O1N anion increased strongly in cationic micelles as compared to a MeCN−H_2O mixture (2:1 v/v, $\tau_0' = 10.8$ ns). Contrary, the fluorescence maximum for this anion was only slightly sensitive to the environment. This suggested that some other factors besides the polarity of the microenvironment could contribute to an increase in the anion lifetime.

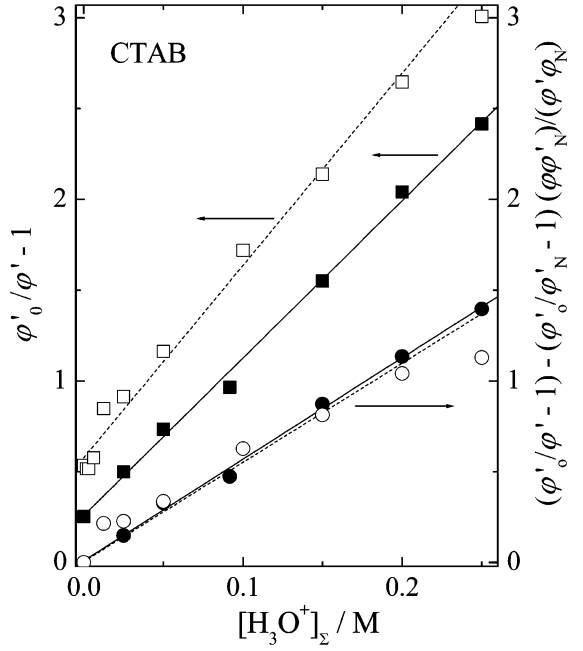

Figure 4. Plots of $\varphi_0'/\varphi' - 1$ (squares) and $(\varphi'_0/\varphi' - 1) - (\varphi'_0/\varphi'_N - 1)(\varphi\varphi'_N)/(\varphi'\varphi_N)$ (circles) vs. $[H_3O^+]_\Sigma$ for 1N (filled symbols) and 2O1N (open symbols) in 50 mM CTAB micellar solution.

The photodissociation rate constant (k_1) was determined from the $*ArO^-$ fluorescence quantum yield and the *ArOH fluorescence decay time at pH ≈ 7 (eq A13). The k_1 value was also estimated from I_N'/I_N by using an intensity ratio $(I_0'/I_0)_S$ measured under conditions of direct excitation of ArO^- and ArOH in ethanol (eq A14). The sum of the apparent rate constants of $*ArO^-$ protonation (k_{-1}) and proton-induced quenching (k_q') was obtained from the fluorescence quantum yields plotted against $[H_3O^+]_\Sigma$ according to eq A9 (see Figure 3a). Values of 12.1 and 9.1 M^{-1} were obtained for $(k_{-1} + k_q')\tau_N'$ in CTAB micellar solutions of 1N and 2O1N. Figure 3b presents the plots in the coordinates corresponding to eq A10. Negative intercepts for these plots were interpreted as negligible rates of the proton-induced fluorescence quenching (k_q) for neutral species of both compounds. Time-resolved fluorescence data for 1N confirm this conclusion on negligible k_q in cationic micelles; values of $(1/\tau_1 + A/\tau_2)/(1 + A) = 1/\tau_0 + k_d + k_1 + k_q[H_3O^+]_\Sigma$ (see eq A5, data not shown) were found to be constant over the entire range of HCl concentration studied. The values of the apparent bimolecular rate constants determined from steady-state and time-resolved data were in good agreement (see Table 1). Similar values of k_{-1} and k_q' were obtained from the $*ArO^-$ fluorescence quantum yields plotted against the proton concentration according to eqs A11 and A12. Good linear correlations for these data (see Figure 4) provided additional evidence for the negligible rate of the proton-induced fluorescence quenching for neutral species in CTAB solutions.

Nonionic Micelles of Brij 35. Figure 5 shows fluorescence spectra of 1N and 2O1N in 10 mM Brij 35 solutions at various HCl concentrations. At pH ≈ 6, the I_N'/I_N ratio for both compounds was much smaller than that in the CTAB solution. The I_N'/I_N values in Brij 35 micelles were comparable to those obtained in 66 vol % aqueous acetonitrile (1.8 and 0.9 for 1N and 2O1N, respectively). An increase in the acid concentration led to effective quenching of ArOH and ArO^- fluorescence (λ_{fl} = 443 and 475 nm for 1N and 2O1N, respectively). In a Brij 35 solution with pH ≈ 6, fluorescence of the neutral form of

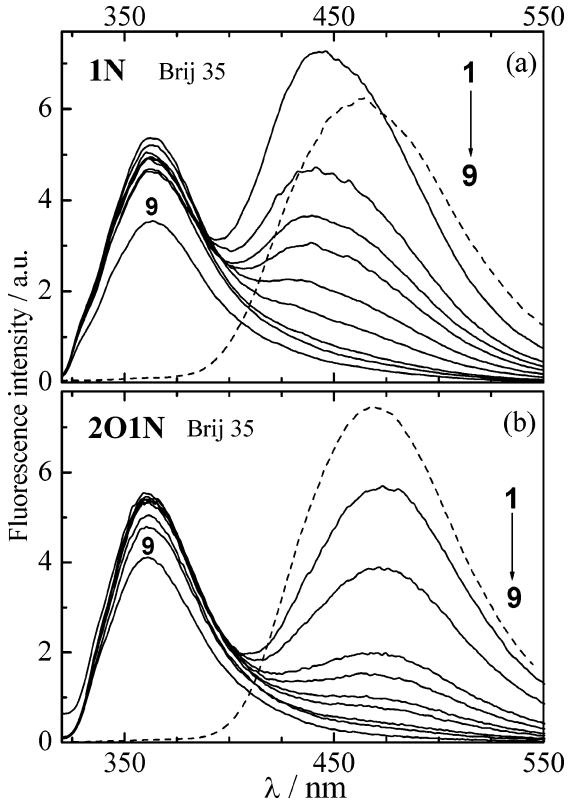

Figure 5. Fluorescence spectra of 1N (a) and 2O1N (b) in 10 mM Brij 35 micellar solution in the presence of NaOH (pH ≈ 13, dashed lines) or HCl (solid lines). Arrows with numbers refer to $*ArO^-$ fluorescence and represent an increase in HCl concentration, which was 0 (1), 5 (2), 8 (3), 13 (4), 25 (5), 50 (6), 150 (7), 250 (8) and 1000 mM (9) for 1N and 0 (1), 5 (2), 17 (3), 25 (4), 50 (5), 83 (6), 200 (7), 500 (8) and 1000 mM (9) for 2O1N. The spectra of basic solutions were multiplied by a factor of 0.5.

1N ($\lambda_{fl} = 363$ nm) decayed exponentially with a lifetime of 2.1 ns (Figure 6). Fluorescence response function of the 1N anion was well described by a two-exponential function (eq A2). The rise and decay time were found to be 1.7 ns and 15.2 ns. In contrast to CTAB solutions, the $*ArO^-$ fluorescence decay in basic Brij 35 solution (pH ≈ 12 in Figure 6) could only be fitted with a sum of two exponentials with decay times of 6.7 ns and 15.4 ns. A substantial decrease of the $*ArO^-$ fluorescence quantum yield and a red shift of the emission maximum (see Figure 5) were observed under basic conditions. The short-living component in the $*ArO^-$ fluorescence decay observed in the basic Brij 35 solutions was ascribed to emission of the anion localized in the aqueous phase. For 2O1N, the $*ArO^-$ decay was found to be monoexponential and the emission maximum to be constant at all pHs studied. These data suggested localization of the neutral and anionic species of this hydrophobic compound in the micellar phase formed by the nonionic surfactant Brij 35.

Noncomplete solubilization of the 1N anion in the micellar phase makes impossible the correct determination of φ_0' for this compound. Fluorescence data obtained for the neutral Brij 35 solution and ethanol were used to estimate k_1 according to eq A14. Feasibility of this procedure is proven by similar values of k_1 obtained with the two methods (eqs A13 and A14) for both naphthols in CTAB solutions and for 2O1N in Brij 35 solution (see Table 1). Figure 7a presents the plots of the fluorescence quantum yield ratio $(\varphi\varphi_N')/(\varphi_N\varphi')$ against $[H_3O^+]_\Sigma$ in Brij 35 micellar solutions. In contrast to the CTAB solutions, these plots were nonlinear. Sublinear dependences may be interpreted in terms of variations of the equilibrium constant for the hydronium ion exchange between the aqueous and micellar phases. This constant should decrease with the acid concentration because of electrostatic repulsive interactions between

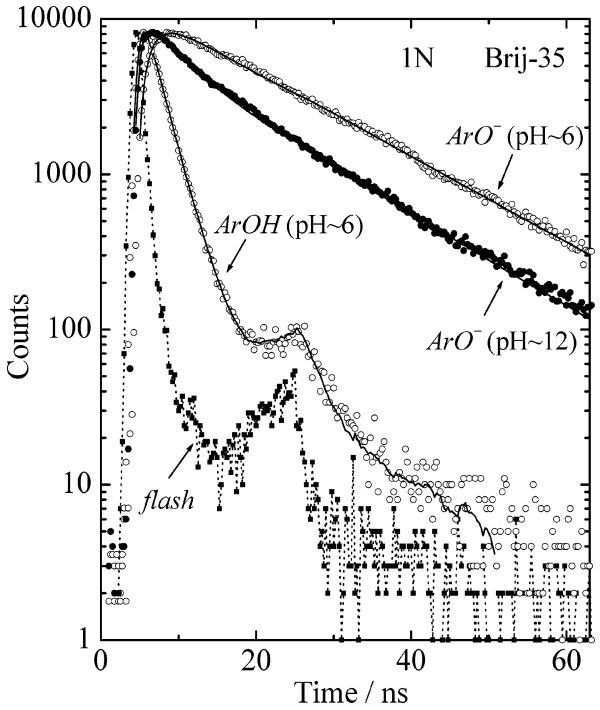

Figure 6. Fluorescence decay curves of the neutral and anionic species of 1N in Brij 35 micellar solution at pH ≈ 6 (open symbols) and 12 (filled symbols). The solid lines are the best fits to the data convoluted with the instrument response function labeled as "flash" (dotted line with symbols).

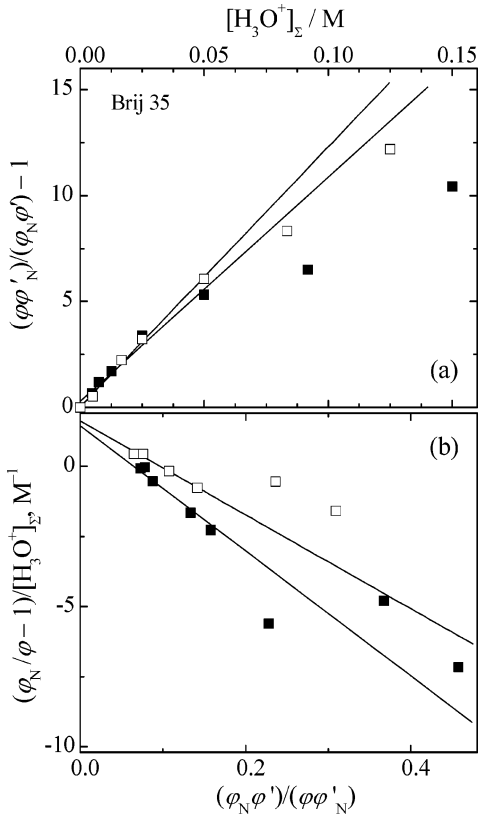

Figure 7. Plots of $(\varphi\varphi_N')/(\varphi_N\varphi') - 1$ vs $[H_3O^+]_\Sigma$ (a) and $(\varphi_N/\varphi - 1)[H_3O^+]_\Sigma$ vs $(\varphi_N\varphi')/(\varphi\varphi_N')$ (b) for 1N (filled symbols) and 2O1N (open symbols) in 10 mM Brij 35 micellar solution.

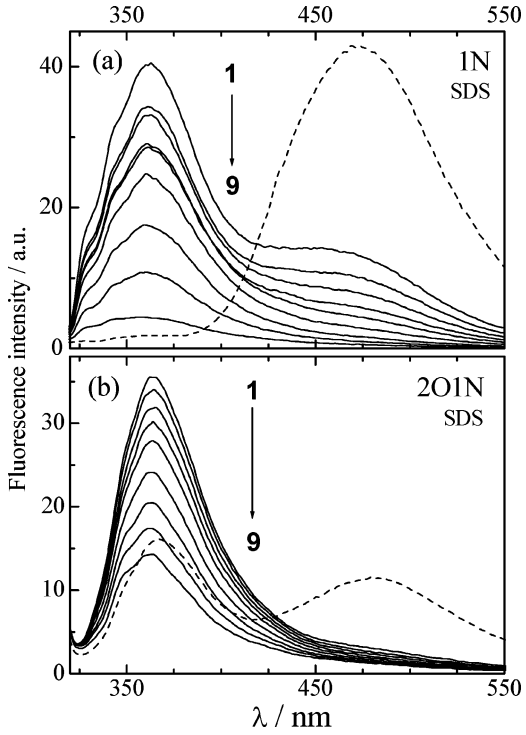

Figure 8. Fluorescence spectra of 1N (a) and 2O1N (b) in 100 mM SDS micellar solution in the presence of NaOH (pH ≈ 13, dashed lines) or HCl (solid lines). Arrows with numbers refer to $*ArO^-$ fluorescence and represent an increase in HCl concentration, which was 0 (1), 1.2 (2), 2.5 (3), 4.2 (4), 6.7 (5), 17 (6), 25 (7), 58 (8) and 250 mM (9) for 1N and 0 (1), 1.6 (2), 3.2 (3), 6.3 (4), 12.5 (5), 25 (6), 50 (7), 100 (8), and 250 mM (9) for 2O1N.

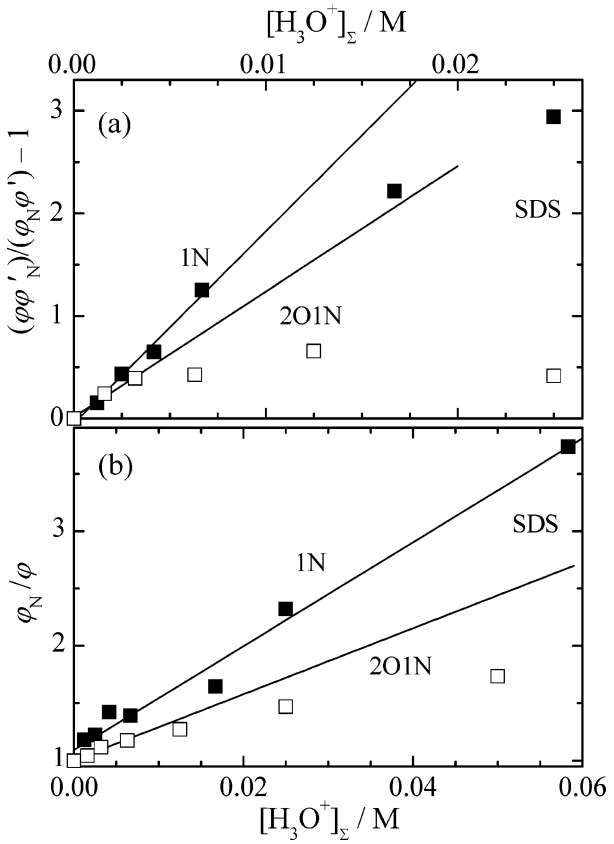

Figure 9. Plots of $(\varphi\varphi_N')/(\varphi_N\varphi') - 1$ vs $[H_3O^+]_\Sigma$ (a) and φ_N/φ vs $[H_3O^+]_\Sigma$ (b) for 1N (filled symbols) and 2O1N (open symbols) in 100 mM SDS micellar solution.

hydronium ions and Brij 35 micelles charged by protons absorbed. The initial slopes ($[H_3O^+]_\Sigma$ < 25 mM) gave $(k_{-1} + k_q')\tau_N'$ values of 106 and 123 M^{-1} for 1N and 2O1N, respectively. The same procedure as for CTAB micelles was used to determine separately all bimolecular rate constants. The values obtained from the fluorescence quantum yields agreed well with the values determined from parameters of fluorescence decay curves measured as a function of the proton concentration (see Table 1).

Anionic Micelles of SDS. Fluorescence spectra of 1N and 2O1N in 100 mM SDS micellar solution are presented in Figure 8. Only very weak emission of anionic species was observed in the fluorescence spectrum of 2O1N (Figure 8b). An increase of τ_N and a decrease of I_N'/I_N in SDS micelles as compared to CTAB and Brij 35 solutions indicated that the protolytic photodissociation slowed when the interfacial electrostatic potential was switched to a negative value. Noncomplete solubilization of the 1N anion was observed in SDS solutions at pH > 11. This was evident from the emission maximum of the 1N anion ($\lambda_{fl} = 472$ nm) that was close to that in bulk water even at pH ≈ 7 and the biexponential decay of $*ArO^-$ fluorescence. In contrast, fluorescence decay curves for anionic species of 2O1N remained single exponential at all pHs studied. Complete dissociation of 2O1N in the ground state could not be observed because of SDS coagulation at pH > 13. All these effects made impossible determination of φ_0' for both compounds in SDS micelles. The k_1 values estimated from the I_N'/I_N ratio according to eq A14 are presented in Table 1.

Figure 9a shows the *ArOH-to-$*ArO^-$ fluorescence quantum yield ratio, which is plotted in the coordinates corresponding to eq A9. The plots for both naphthols in SDS micelles strongly deviated from linearity. These results were interpreted in much the same manner as it was done for Brij 35 micelles; absorption of hydronium ions by micelles resulted in a change of the surface potential and, therefore, in a decrease of the activity coefficient of H_3O^+ and of the apparent rate constants. Similar sublinear plots have also been observed for the proton-induced fluorescence quenching of 1-substituted naphthalenes in SDS micelles.[41] The latter results have been described by the ion exchange formalism. In this work, only initial slopes were used to estimate $(k_{-1} + k_q')\tau_N'$. Values of 187 and 122 M^{-1} were obtained for 1N and 2O1N, respectively. Separate determination of k_{-1} and k_q' was done only for 1N by using parameters of fluorescence decay curves measured as a function of HCl concentration. Plots in the coordinates corresponding to eqs A3−A7 were also strongly nonlinear, and only initial slopes were used. As can be seen from Figure 8, strong proton-induced quenching of *ArOH fluorescence was observed in the anionic micelles. The *ArOH fluorescence quenching rate could be easily determined from the plot of φ_N/φ vs acid concentration (the second term in the right part of eq A10 could be neglected because the photodissociation rate in the SDS micelles was relatively small).

Discussion

The proton-transfer kinetics in micellar solutions is strongly affected by the rate of reactants' migrations between the micellar and aqueous phases. In our previous studies,[16−19] we have shown that many aromatic hydroxycompounds in the ground and excited state could be almost completely solubilized in the micellar phase, i.e., the rate of *ArOH exit from the micellar phase was much smaller than the fluorescence decay rate. The exit of aromatic anions ($*ArO^-$) from the micellar phase into the aqueous phase was found only in like charged anionic micelles.[16c,d] The rate constant for the exit of the excited anions

SCHEME 2

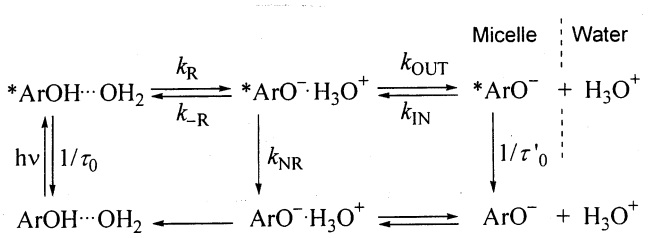

of chlorosubstituted 2-naphthols from SDS micelles was estimated to be $\sim$0.1 ns^{-1}. Even in this case, the exit was rather slow to affect substantially the rate and equilibrium constant values determined from fluorescence quantum yield and/or fluorescence decay measurements. The interphase exchange rate for other reactants, particularly for hydronium ions, should be high, and it is, therefore, very important to take it into account in analyzing proton-transfer dynamics in micelles.

Our data for k_1, k_{-1}, and pK* in micellar solutions are collected in Table 1. Kinetics of the protolytic reactions in micelles was rationalized in terms of a simple model including an intramicellar proton-transfer equilibrium and interfacial exchange of hydronium ions (Scheme 2).

Scheme 2 is formally quite similar to a kinetic scheme commonly used for homogeneous solutions.[33,42,43] Here, k_R and k_{-R} are the rate constants of the forward and backward proton transfer along hydrogen bonds in reactive complexes, k_{NR} is the rate constant of radiationless decay of a reactive ion pair. The rate constants k_{IN} and k_{OUT} refer to formation and separation of the ion pair inside the micellar phase. It must be emphasized that k_{IN} and k_{OUT} correspond to interfacial exchange processes. In contrast, the analogous parameters, k_{REC} and k_{SEP}, for a reaction in homogeneous solution refer to the rate constants obtained from the steady-state approximation for diffusion. Nonstationary effects related to geminate recombination seem to be of minor importance and can be neglected for many photoacids and photobases. However, these effects are essential for kinetic studies in the picosecond time domain and they can be used to unravel some mechanistic details.[42−45]

Apparent rate (k_1) and equilibrium ($K^* = k_1/k_{-1}$) constants for the excited-state protolytic dissociation in micelles can be written as

$$k_1 = \frac{k_R k_{OUT}}{k_{-R} + k_{NR} + k_{OUT}} = \frac{k_{IN} K^*}{1 + (k_{NR} + k_{OUT})/k_{-R}} \quad (2)$$

$$k_{-1} = \frac{k_{-R} k_{IN}}{k_{-R} + k_{NR} + k_{OUT}} = \frac{k_{IN}}{1 + (k_{NR} + k_{OUT})/k_{-R}} \quad (3)$$

$$K^* = k_1/k_{-1} = (k_R/k_{-R})\,(k_{OUT}/k_{IN}) \quad (4)$$

Experimental values of pK* for 1N and 2O1N in CTAB, Brij 35, and SDS micelles were very close to each other. This indicates that the presence of the alkyl substituent did not result in a significant change of the localization of the reactive group so that the ratio (k_R/k_{-R}) did not differ much for these two compounds. Somewhat different effects have been observed for 2N derivatives.[24] In CTAB micelles, the pK* value was larger by $\sim$0.5 unit for alkyl-substituted 2N than for the parent compound. This has been explained by a different localization (orientation) of the alkyl substituted compounds in the CTAB micelles that resulted in largely different energies of anion solvation. Quantum efficiencies of the protolytic photodissociation (η) and of the adiabatic protonation of *ArO$^-$ by hydronium ions (η') can be expressed as

$$\eta = k_1/(k_1 + k_d) = k_{OUT}/(k_{OUT} + k_{NR}) \quad (5)$$

$$\eta' = k_{-1}/(k_{-1} + k'_q) = k_{-R}/(k_{-R} + k_{NR}) \quad (6)$$

These quantum efficiencies were determined from experimental data (see eqs A15 and A16) and used further to evaluate some rate constants introduced in Scheme 2. Values of k_{NR}/k_{OUT}, k_{NR}/k_{-R}, and k_{-R}/k_{OUT} were obtained by using eqs 5 and 6. These ratios of the rate constants were utilized to calculate k_R and k_{IN} from the values of k_1 and k_{-1} according to eqs 2 and 3. The results are presented in Table 1.

A shift of apparent pK* in micellar solutions (pK^*_m) relative to that in bulk water (pK^*_w) was observed for 1N derivatives (Table 1) and other hydroxyaromatic compounds.[14−24,46] According to eq 4, the pK* difference can expressed in the following form

$$\Delta pK = pK^*_m - pK^*_w = \log [(k_{IN}/k_{OUT})/(k_{REC}/k_{SEP})] - \log [(k_R/k_{-R})_m/(k_R/k_{-R})_w] \quad (7)$$

pK* values of 1N and 2O1N in nonionic micelles appeared to be very close to those in MeCN$-$H$_2$O mixture (2:1 v/v). This implies similar values of k_R/k_{-R} provided that the diffusion parameters (k_{IN}/k_{OUT} and k_{REC}/k_{SEP}) are not substantially different in these media. The pK* shift in aqueous acetonitrile was shown to be mainly caused by a ca. 40-fold decrease of k_R.[33] This effect was only partly compensated by an increase of k_{SEP}/k_{REC}. A comparable decrease of k_R might be anticipated in micelles. Data in Table 1 show that k_R values in the micellar solutions are indeed very close to those in the MeCN$-$H$_2$O mixture. Notice that k_1 in the series CTAB, Brij 35, and SDS showed much larger variations than k_R. In cationic micelles of CTAB, the apparent pK* value of 1N was found to be smaller by $\sim$2 units than that in nonionic micelles. The excited-state acidity of this compound in cationic micelles was even greater than in aqueous solution.[14−24,46] When Brij 35 micelles were compared to anionic micelles of SDS, a smaller increase by $\sim$1 unit was found for 1N. Its ground-state pK increased only by 1 unit in the series CTAB, Brij 35, SDS. In contrast, comparable variations by more than 3 units were observed for pK* and pK of 2O1N in these micellar solutions.

To gain a better understanding of micellar effects on the protolytic dissociation, we converted our pK data into micellar surface potentials, which should be independent of a probe used. The interfacial electrostatic potential (ψ) can be calculated from the pK shift according to eq 8[13−15]

$$\psi = \frac{2.303RT}{F}\,\Delta\Delta pK, \quad (8)$$

where $\Delta\Delta pK = \Delta pK(\psi) - \Delta pK(0) = pK_m(\psi) - pK_m(0)$. Here, p$K_m$(0) was taken to be equal to a value in neutral Brij 35 micelles. The micellar surface potentials obtained from our data for 1N derivatives are presented in Table 2. For comparison, the ψ values were also estimated from ground-state titration data for ω-(2-hydroxynaphthyl-1)-decanoic acid.[47] The ψ values obtained with the use of the strongly hydrophobic 2O1N are in good agreement with one another and with data reported for CTAB and SDS micelles at the ionic strength used.[14,15,21,48]

Discrepancies in ΔpK observed for the singlet excited and ground state of 1N as compared to 2O1N were attributed to an implicit difference in the meaning of pK and pK*. The ground-state pK obtained from the spectrophotometric titration corre-

TABLE 2: Micellar Surface Potentials Calculated from the Ground- and Excited-State p*K* Values of Naphthols[a]

probe	state[b]	CTAB	Brij 35[c]	SDS
2-octadecyl-1-naphthol	G	+95 (10.0)	0 (11.6)	<−83 (>13)
	E	+106 (−0.7)	0 (1.1)	−112 (3)
1-naphthol	G	+35 (9.5)	0 (10.1)	−24 (10.5)
	E	+101 (−0.6)	0 (1.1)	−71 (2.3)
ω-(2-hydroxynaphthyl-1)-decanoic acid	G	+89 (10.0)	0 (11.5)	−18 (11.8)

[a] Electrostatic potentials are given in mV; numbers in the brackets are p*K* values. [b] Letters "G" and "E" refer to the ground- and excited-state data. [c] Zero value of the surface potential was assigned to Brij 35 micelles.

sponds to an equilibrium established for all reagents. This quantity in micellar solutions can be expressed as

$$pK_m = -\log \frac{[ArO^-]_w \rho_A [H_3O^+]_w \rho_H}{[ArOH]_w \rho_{AH}} = pK_w - \log \frac{\rho_A \rho_H}{\rho_{AH}} \approx pK_w - \log \rho_A^{el} \rho_H \quad (9)$$

where ρ_{AH}, ρ_A, and ρ_H are the distribution coefficients between the micellar and aqueous phase for ArOH, ArO^-, and H_3O^+, respectively. An approximate equality was obtained by assuming that $\rho_A \approx \rho_{AH}\rho_A^{el}$, where ρ_A^{el} is the electrostatic contribution to the distribution coefficient of ArO^-. The ground-state p*K* shift depends largely on the distribution coefficients of ArO^- and H_3O^+. In contrast, the excited-state p*K** is obtained from the rate constant ratio (k_1/k_{-1}) under steady-state conditions and assumptions that *ArOH and *ArO^- are completely solubilized in the micellar phase. Thus, p*K** shift depends only on the interfacial distribution of H_3O^+ and does not depend on the interfacial equilibrium for *ArOH and *ArO^-. For highly hydrophobic compounds, the electrostatic contribution to ρ_A can be neglected and, therefore, both p*K* and p*K** depend mainly on the distribution of H_3O^+, which is largely governed by electrostatics. Very good agreement between micellar surface potentials calculated from p*K* and p*K** values of 2O1N confirmed this conclusion. The p*K** values for 1N also provided reasonably good estimates for the micellar potential, although a significantly smaller ψ value for SDS micelles indicated that the excited anion of 1N leaves the negatively charged micelles. Ground-state p*K* values for 1N and *ω*-(2-hydroxynaphthyl-1)-decanoate gave very small values of the surface potential of SDS micelles. This showed that their deprotonated forms are localized in the aqueous phase.

A deeper insight into mechanisms of the protolytic reactions in micelles can be gained from analysis of a correlation between k_1 and *K** for a set of compounds in micelles of a certain charge type. From eq 2, one can easily obtain the following relation

$$\log(k_1/s^{-1}) = \log(k_{IN}/s^{-1}) - pK^* - \log(1 + (k_{NR} + k_{OUT})/k_{-R}) \quad (10)$$

Nonradiative deactivation (k_{NR}) is negligible for the majority of aromatic compounds in aqueous solutions. Although the rate of this process for 1N derivatives in water and in micelles appeared to be comparable with the diffusion-controlled separation of the ion-pair (see Table 1 and refs 33 and 44), the term k_{NR}/k_{-R} was still smaller than k_{OUT}/k_{-R} for these systems. If we neglect the radiationless decay of the reactive ion-pair, we can rearrange eq 10 to

$$\log(k_1/s^{-1}) = \log(k_{IN}/k_{OUT}) - pK^* - \log([1/k_{-R}+1/k_{OUT}]/s) \quad (11)$$

The rate constant k_{-R} can be expressed as a function of p*K** by using the following expressions

$$k_{-R} = k_R \exp(\Delta G/RT) = k_R^\circ \exp[(\Delta G - \Delta G^\ddagger)/RT] \quad (12)$$

$$\Delta G = 2.3RT[pK^* - \log(k_{IN}/k_{OUT})] \quad (13)$$

$$\Delta G^\ddagger = \Delta G/2 + [(\Delta G/2)^2 + (\Delta G_0^\ddagger)^2]^{1/2} \quad (14)$$

where ΔG and $\Delta G^\ddagger$ are the reaction and activation free energies for intramicellar proton transfer with the rate constant k_R and $\Delta G_0^\ddagger$ is the activation energy of the isoergonic reaction ($\Delta G = 0$ and $k_R = k_{-R}$).[49] Combining eqs 11−14 we obtained

$$\log(k_1/s^{-1}) = a - pK^* - \log\{\exp[1.151(a-pK^*) + (1.325(a - pK^*)^2 + b^2)^{1/2}]/\exp[2.303c] + \exp[-2.303d]\} \quad (15)$$

where $a = \log(Mk_{IN}/k_{OUT})$, $b = \Delta G_0^\ddagger/RT$, $c = \log(k_R^0/s^{-1})$, and $d = \log(k_{OUT}/s^{-1})$. For the reactions in water, $a = \log(Mk_{REC}/k_{SEP})$ and $d = \log(k_{SEP}/s^{-1})$. Experimental data obtained in this work and found in the literature[6,7,15−17,44,50−57] for water, cationic micelles (CTAB, tetradecyltrimethylammonium bromide, and dodecylpyridinium chloride), and nonionic micelles (Brij 35, 56, and 58) are presented in Figure 10. It should be emphasized that experimental data both for the ground-state and excited-state reactions were used in the same plots. For aqueous solutions, we simultaneously analyzed data for acids of different charge. As one can see from Figure 10, variations in k_1 and p*K* caused by the electrostatic effects on the diffusion rate constants appeared to be relatively small and comparable to variations caused by other (unknown) factors. Results of fitting the kinetic data to eq 15 are collected in Table 3. Generally, good description within the formalism presented above was achieved for the reactions in micelles and aqueous solutions.

When we used four-variable parameters in fitting the data for homogeneous aqueous solution, we obtained $\Delta G_0^\ddagger/RT \approx 0$ and $\log(k_R^0/s^{-1}) = 11.3 \pm 0.3$. This means that the limiting rate of proton transfer is characterized by a time of 3−10 ps ($1/k_R^0$), which coincides with the dielectric relaxation time of water ($\tau_D = 8-9$ ps)[58] within the accuracy of the analysis. It is generally believed that the intrinsic barrier for proton transfer between heteroatoms is very small.[50,59] Very high uncertainty (several orders of magnitude) in the $\Delta G_0^\ddagger/RT$ value obtained in our analysis precludes further discussion of this quantity. When we fitted the data using k_{IN} and k_{OUT} fixed to the values calculated for the diffusion-controlled reaction of a monoanion with H_3O^+ (see Table 3 and ref 33), we obtained practically the same values of the intrinsic barrier and the limiting rate constant. These parameters were found to be quite different in cationic micelles. Of special interest is an approximately 60-fold decrease in k_R^0. This change is accompanied by an increase in the activation free energy of the isoergonic reaction. The

TABLE 3: Kinetic Parameters Obtained by Fitting Eq 15 to the Data Shown in Figure 10a[a]

	$\log(k_R^0/s^{-1})$	$\Delta G_0^{\ddagger}/RT$	$\log(Mk_{IN}/k_{OUT})$	$\log(k_{OUT}/s^{-1})^b$	$\log(k_{IN}/M^{-1}\ s^{-1})^b$
water	11.3 (11.3)[b]	0 (0)	0.0 (−0.3)	10.6 (10.9)	10.8
cationic micelles	11.2 (9.46)	5.3 (1.5)	0.1 (0.14)	9.5 (22.5)	9.6
nonionic micelles	11.2	7.7	1.7	8.9	10.6

[a] The rate constants for diffusion-controlled steps were kept constant and equal to the calculated values shown. Values in the brackets were obtained by using four variable parameters. [b] For water, k_{IN} and k_{OUT} correspond to the steady-state diffusion rate constants denoted as k_{REC} and k_{SEP}. For uniformly reactive spheres, the following equations were used: $k_{IN} = k_{REC} = [4\pi N_A aD/1000][\delta/(e^{\delta} - 1)]$, $k_{OUT} = k_{SEP} = [3D/a^2][\delta/(1 - e^{-\delta})]$, where $\delta = -e^2/(4\pi\epsilon_o\epsilon\ a\ RT)$, $D = 1.0 \times 10^{-4}$ cm^2/s, $T = 295$ K, $\epsilon = 78$, and $a = 7$ Å for water; $\delta = \psi F/RT$, $a = 27$ Å, and $\psi = 0$ and +100 mV for nonionic and cationic micelles, respectively. For diffusion-controlled reactions of a uniformly reactive sphere B with radius R_B and a sphere A with radius R_A that has a reactive hemisphere with radius l_A, the rate constants calculated for micelles were multiplied by a steric factor (f) of 0.19, that was estimated using eqs 6, 19, and 20 from ref 60; $R_A = 20$ Å, $R_B = 1$ Å, $l_A = 7$ Å. Only minor changes in f were obtained when R_B was varied from 1 to 5 Å.

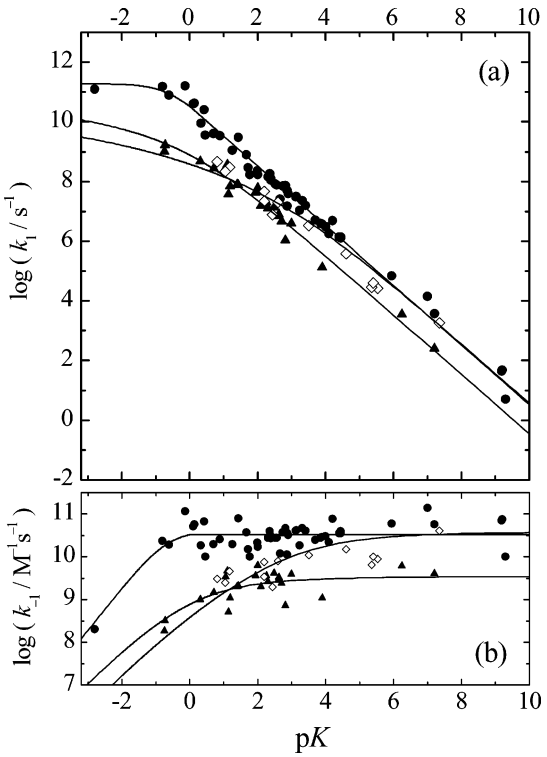

Figure 10. Plots of $\log(k_1/s^{-1})$ (a) and $\log(k_{-1}/M^{-1}\ s^{-1})$ (b) vs pK* in aqueous solution (circles), cationic micelles (triangles), and nonionic micelles (diamonds). Solid lines correspond to the fitting curves obtained by using eq 15. Fitting parameters are presented in Table 3.

fitting results for cationic micelles showed that the rate constant of the diffusion-controlled separation of the ion pair (k_{OUT}) was indeterminate (a fitting error of $\sim 10^{12}$ for $\log(k_{OUT}/s^{-1})$. If we assume that the reaction of a naphtholate anion buried in a micelle and a hydronium ion can be modeled by a diffusion-controlled reaction of two uniformly reactive spheres with radii of ~20 Å (micelle) and 7 Å (proton), we obtain unrealistically large values of the diffusion rate constants ($\log k_{IN} = 11.3$ and 10.3 for nonionic and cationic micelles, see Table 1 and footnote for Table 3). To obtain more reasonable estimates for these quantities, we used approximate relations[60] for a steric factor derived for the diffusion-controlled reactions of one uniformly reactive molecule (proton) with another one having a reactive hemisphere (micelle with naphthol). This model seems to provide more accurate parameters than the more popular model of reactive patches.[61] The model parameters used can be found in Table 3. The calculated rate constants for anisotropic diffusion were in reasonable agreement with k_{IN} estimated from experimental data for cationic and nonionic micelles (see Tables 1 and 3). Fitting the data for cationic micelles with the diffusion rate constants as fixed parameters yielded a $\Delta G_0^{\ddagger}/RT$ value of 5.3 and the limiting rate of proton transfer similar to that in water. The latter result suggests similarity of dielectric relaxation times in these media, which is also supported by available experimental data for mixed MeCN solutions.[62] $k_R = 2$ ns^{-1} and $k_{-R}/k_{OUT} = 0.1$ calculated from the fitting parameters for an acid with p$K = -0.7$ also compare well with the experimental results for 1N and 2O1N in CTAB micelles (Table 1). We used k_R^0 and $\Delta G^{\ddagger}_0/RT$ obtained by fitting the data for cationic micelles together with k_{IN} and k_{OUT} calculated for a ψ value of −100 mV to calculate k_R and k_{-R} for an acid with pK = 3 in anionic micelles. Although we could not reproduce the absolute values obtained for 2O1N in SDS micelles, the calculated parameters showed the same tendency as seen for this compound in CTAB and SDS micelles. The lack of the data for pK < 1 in nonionic micelles prevents independent estimation of all four parameters. When we used the calculated values of the diffusion rate constants and k_R^0 obtained for cationic micelles as fixed parameters, we obtained $\Delta G^{\ddagger}_0/RT = 7.7$.

Analysis of experimental data for homogeneous aqueous solution showed that, for compounds with pK > 0, $k_{-R} \gg k_{SEP}$ and k_{NR}, and therefore, reaction kinetics is mainly controlled by the protolytic equilibrium in the solvent cage and by the proton diffusion rate

$$k_1 = \frac{k_R k_{SEP}}{k_{-R} + k_{NR} + k_{SEP}} \approx (k_R/k_{-R})k_{SEP} \qquad (16)$$

$$k_{-1} = \frac{k_{-R} k_{IN}}{k_{-R} + k_{NR} + k_{SEP}} \approx k_{IN} \qquad (17)$$

In micellar solutions, this kinetic regime appears to be realized only for very weak acids (pK > 5). For the vast majority of photoacids, the protonation rate (k_{-R}) is comparable to the diffusion-controlled rate of the proton exit (k_{OUT}) and the plots of $\log(k_1/s^{-1})$ vs pK* are expected to be essentially nonlinear. For compounds with pK* < 1, the photodissociation rate constant (k_1) in cationic micelles should be close to the rate constant of proton-transfer inside a micelle (k_R) and it may be used to directly characterize water properties in the micellar interior.

Figure 10 shows that kinetic data for long-chain substituted naphthols fit in with the common picture of the protolytic dissociation of aromatic compounds. There is hardly any specific effect of hydrophobicity on the kinetic parameters. The steric hindrance plays an important role in cluster experiments where one can measure high-resolution spectra of ArOH−A$_n$ isomers where A is a proton acceptor.[63] However, studies in liquid solution deal with the statistical distribution of all possible conformers and aggregates. Our experimental findings in homogeneous solutions[33] as well as in micelles demonstrate that

excited-state proton-transfer rates are somewhat smaller for 2O1N than for 1N but not much, probably because of nature of water cluster as proton acceptor. The *o*-alkyl group seems not to disrupt $(H_2O)_n$ and $(H_2O)H^+_n$ structures critically. In nonionic micelles, p*K** and k_1 for 1N and 2O1N are practically identical and close to the corresponding quantities in aqueous acetonitrile solution.[33] Only minor discrepancies between acidity constants and rate constants of 1N and its hydrophobic analogue were observed in cationic micelles. This suggests similar average localization sites for the hydroxy group of 1-naphthol and its hydrophobic derivative inside the micellar phase. The conclusion is supported by our NMR studies that showed similar localization of naphthols and their alkyl derivatives in CTAB micelles.[64]

Conclusions

2-Octadecyl-1-naphthol in the ground state was found to be a weaker acid than the parent compound in micellar solutions. In the singlet excited state, 1-naphthol and its octadecyl derivative showed similar rate and equilibrium constants of the protolytic dissociation in CTAB and Brij 35 micelles. Although the long-chain alkyl group appeared to have little effect, if any, on the 1-naphthol localization in micelles, hydrophobic derivatives are clearly better probes for negatively charged systems, and they can provide further insights into mechanisms of proton-transfer reactions in surfactant assemblies.

A comparative study of the excited-state proton-transfer reaction of naphthols and their long-chain derivatives allowed proposing a kinetic model of the reaction in micellar solution. The central point of the model is the direct proton exchange between micellar and aqueous phases that is strongly dependent on the micellar surface potential. Analysis of the correlation between rate constants and p*K* for various compounds suggested significant differences in the mechanisms of the protolytic dissociation in water and in micellar solutions. Available experimental data for cationic and nonionic micelles can be rationalized if one considers anisotropic reactivity for diffusion-controlled steps and assumes much higher intrinsic barrier (or lower limiting rate) for the proton-transfer step in the micellar interior.

Appendix

Excited-state proton-transfer reactions in micellar solutions of 1N derivatives are described by Scheme 1, which is similar to that used for homogeneous solutions.[33] According to this scheme, the fluorescence kinetics of *ArOH (I) and *ArO$^-$ (I') has to obey the following equations

$$I(t) = I_0[\exp(-t/\tau_1) + A\exp(-t/\tau_2)] \quad \text{(A1)}$$

$$I'(t) = I_0'[\exp(-t/\tau_2) - \exp(-t/\tau_1)] \quad \text{(A2)}$$

where

$$1/\tau_{1,2} = (\mu + \mu')/2 \pm [(\mu - \mu')^2/4 + k_1 k_{-1}[H_3O^+]_\Sigma]^{1/2} \quad \text{(A3)}$$

$$A = (1/\tau_1 - \mu)/(\mu - 1/\tau_2) \quad \text{(A4)}$$

$$\mu = 1/\tau_0 + k_d + k_1 + k_q[H_3O^+]_\Sigma = (1/\tau_1 + A/\tau_2)/(1 + A) \quad \text{(A5)}$$

$$\mu' = 1/\tau_0' + (k_{-1} + k'_q)[H_3O^+]_\Sigma = 1/\tau_1 + 1/\tau_2 - \mu \quad \text{(A6)}$$

$$k_1 k_{-1}[H_3O^+]_\Sigma = \mu\mu' - 1/(\tau_1\tau_2) \quad \text{(A7)}$$

One can obtain all rate constants from measured values of τ_1, τ_2, and A if τ_0 and τ'_0 are known. In contrast to homogeneous solutions, where proton activity could be estimated from the concentration, total concentration of an acid added was used as $[H_3O^+]_\Sigma$ in our studies of micellar solutions. All the bimolecular rate constants had therefore apparent values. The rate constants can also be obtained from *ArOH(φ) and *ArO$^-$(φ') fluorescence quantum yields measured as a functions of $[H_3O^+]_\Sigma$, when the data are plotted according to the following equations

$$(\varphi\varphi_0')/(\varphi_0\varphi') = \{1 + (k_{-1} + k_q')\tau_N'[H_3O^+]_\Sigma\}/k_1\tau_0 \quad \text{(A8)}$$

$$(\varphi\varphi'_N)/(\varphi_N\varphi') = 1 + (k_{-1} + k_q')\tau_N'[H_3O^+]_\Sigma \quad \text{(A9)}$$

$$(\varphi_N/\varphi - 1)/[H_3O^+]_\Sigma = k_q\tau_N - k_1\tau_N k_{-1}\tau_0'(\varphi_N\varphi')/(\varphi\varphi_N') \quad \text{(A10)}$$

$$(\varphi_0'/\varphi' - 1) - (\varphi_0'/\varphi_N' - 1)(\varphi\varphi_N')/(\varphi'\varphi_N) = k_q'\tau_0'[H_3O^+]_\Sigma \quad \text{(A11)}$$

$$\varphi_0'/\varphi' - 1 = 1/(k_1\tau) + k_q'\tau_0'[H_3O^+]_\Sigma + (k_{-1} + k_q')\tau_0'[H_3O^+]_\Sigma/(k_1\tau)_\Sigma \quad \text{(A12)}$$

Here, $\varphi_0 = k_f\tau_0$ and $\varphi_0' = k_f'\tau_0'$ are the fluorescence quantum yields of *ArOH and *ArO$^-$ in the absence of the excited-state protolytic reactions, φ_N and φ'_N are the fluorescence quantum yields of *ArOH and *ArO$^-$ measured at pH $\sim$ 7, when all bimolecular processes can be neglected, $1/\tau = 1/\tau_0 + k_d$ and τ_N is the ArOH fluorescence decay time at pH close to neutral. Equations A11 and A12 are valid only if $k_q/k_1 \ll k_q'\tau_0'$.

The photodissociation rate constant (k_1) can be directly estimated from the fluorescence data obtained at pH $\sim$ 7

$$k_1 = (\varphi_N'/\varphi_0')(\tau_0'/\tau_N')/\tau_N \quad \text{(A13)}$$

The fluorescence quantum yield was corrected for a difference in the *ArO$^-$ fluorescence decay times at neutral (τ_N') and basic pH (τ_0'). In some micellar solutions, φ_0' cannot be measured correctly because anionic species in the ground state are localized in the aqueous phase. For such systems, k_1 can be determined from φ_N'/φ_N and the radiative rate constant ratio (k_f'/k_f). The latter quantity is assumed to be insensitive to environment and is evaluated using independent measurements of the fluorescence quantum yields and lifetimes in the absence of proton transfer

$$k_1 = \frac{(\varphi_N'/\varphi_N)}{(\varphi_0'/\varphi_0)_S}\frac{(\tau_0'/\tau_0)_S}{\tau_N'} \quad \text{(A14)}$$

Here, $(\varphi_0'/\varphi_0)_S$ and $(\tau_0'/\tau_0)_S$ are the ratios of the quantum yields and decay times in a selected solvent S, where no excited-state proton transfer takes place.

Quantum efficiency of the adiabatic protolytic dissociation of *ArOH ($\eta = k_1/(k_1 + k_d)$) is calculated according to the following equations

$$\eta = (\varphi_N'/\varphi_0')(\tau_0'/\tau_N')/(1 - \tau_N/\tau_0) \quad \text{(A15)}$$

$$\eta = \frac{(\varphi_N'/\varphi_N)}{(\varphi_0'/\varphi_0)_S}\frac{(\tau_0'/\tau_0)_S}{(1/\tau_N - 1/\tau_0)\tau_N'} \quad \text{(A16)}$$

References and Notes

(1) Mitchell, P. *Chemiosmotic Coupling and Energy Transduction*; Glynn Research: Bodmin, 1968.

(2) Skulachev, V. P. *Membrane Bioenergetics*; Springer-Verlag: Berlin, 1988.
(3) Cramer, W. A.; Knaff, D. B. *Energy Transduction in Biological Membranes*; Springer-Verlag: New York, 1990; Chapter 8.
(4) Saraste, M. *Science* **1999**, *283*, 1488.
(5) For proton transport in bacteriorhodopsin, see: *Biochim. Biophys. Acta* **2000**, *1460*, 1−239 and references therein.
(6) Gutman, M.; Nachliel, E. *Annu. Rev. Phys. Chem*. **1997**, *48*, 329.
(7) Gutman, M.; Nachliel, E. *Biochim. Biophys. Acta* **1995**, *1231*, 123.
(8) Brandsburg-Zabary, S.; Fried, O.; Marantz, Y.; Nachliel, E.; Gutman, M. *Biochim. Biophys. Acta* **2000**, *1458*, 120.
(9) Zundel, G. *Adv. Chem. Phys*. **2000**, *111*, 1.
(10) Steenken, S. *Biol. Chem.* **1997**, *378*, 1293.
(11) Scheiner, S. *Theor. Comput. Chem*. **1999**, *8*, 35.
(12) Gust, D.; Moore, T. A.; Moore, A. L. *Acc. Chem. Res*. **2001**, *34*, 40.
(13) Fendler, J. H. *Membrane Mimetic Chemistry*; Wiley: New York, 1982.
(14) Kalyanasundaram, K. *Photochemistry in Microheterogeneous Systems*; Academic Press: London, 1987.
(15) Kuzmin, M. G.; Zaitsev, N. K. In *The Interface Structure and Electrochemical Processes at the Boundary between Two Immiscible Liquids*; Kazarinov, V. E., Ed.; Springer-Verlag: Berlin, Heidelberg, 1987; p 207 and references therein.
(16) (a) Kuzmin, M. G. In *Supramolecular Chemistry*; Balzani, V., De Cola, L., Eds.; Kluwer: Dordrecht/Boston/London, *NATO ASI Series, Series C* **1992**, *371*, 279−294. (b) Abou-Al Einin, S.; Zaitsev, A. K.; Zaitsev, N. K.; Kuzmin, M. G. *J. Photochem. Photobiol. A* **1988**, *41*, 365. (c) Zaitsev, A. K.; Zaitsev, N. K.; Kuzmin, M. G. *High Energy Chem.* **1986**, *20*, 251.
(17) (a) Il'ichev, Yu. V.; Demyashkevich, A. B.; Kuzmin, M. G. *High Energy Chem.* **1989**, *23*, 343. (b) Il'ichev, Yu. V.; Solntsev, K. M.; Kuzmin, M. G.; Lemmetyinen, H. *J. Chem. Soc., Faraday Trans.* **1994**, *90*, 2717.
(18) Il'ichev, Yu. V.; Demyashkevich, A. B.; Kuzmin, M. G. *J. Phys. Chem.* **1991**, *95*, 3438.
(19) Il'ichev, Yu. V.; Demyashkevich, A. B.; Kuzmin, M. G.; Lemmetyinen, H. *J. Photochem. Photobiol. A* **1993**, *74*, 51.
(20) Il'ichev, Yu. V.; Solntsev, K. M.; Demyashkevich, A. B.; Kuzmin, M. G.; Lemmetyinen, H.; Vuorimaa, E. *Chem. Phys. Lett.* **1992**, *193*, 128.
(21) Solntsev, K. M.; Il'ichev, Yu. V.; Demyashkevich, A. B.; Kuzmin, M. G. *J. Photochem. Photobiol. A* **1994**, *78*, 39.
(22) Il'ichev, Yu. V.; Shapovalov, V. L. *Bull. Russ. Acad. Sci., Chem. Sci.* **1992**, *41*, 1762.
(23) Hansen, J. E.; Pines, E.; Fleming, G. R. *J. Phys. Chem*. **1992**, *96*, 6904.
(24) Cohen, B.; Huppert, D.; Solntsev, K. M.; Tsfadia, Y.; Nachliel, E.; Gutman, M. *J. Am. Chem. Soc.* **2002**, *124*, 7539.
(25) Silber, J. J.; Biasutti, A.; Abuin, E.; Lissi, E. *Adv. Colloid Interface Sci*. **1999**, *82*, 189.
(26) Bhattacharyya, K. *Acc. Chem. Res.* **2003**, *36*, 95.
(27) Selinger, B. K.; Weller, A. *Aust. J. Chem*. **1977**, *30*, 2377.
(28) Harris, C. M.; Selinger, B. K. *Z. Phys. Chem. (Wiesbaden)* **1983**, *134*, 65.
(29) Mandal, D.; Pal, S. K.; Bhattacharyya, K. *J. Phys. Chem. A* **1998**, *102*, 9710.
(30) Ramamurthy, V. *Photochemistry in Organized and Constrained Media*; VCH: New York−Weinheim, 1991.
(31) Haughland, R. P. *Handbook of Fluorescence Probes and Research Chemicals*; Molecuar Probes: Eugene, 1996.
(32) Levinger, N. E. *Curr. Opin. Coll. Interface Sci*. **2000**, *5*, 118.
(33) Solntsev, K. M.; Abou Al-Ainain, S.; Il'ichev, Yu. V.; Kuzmin, M. G., in preparation.
(34) (a) Pines, E.; Fleming, G. R. *Chem. Phys*. **1994**, *183*, 393. (b) Pines, E.; Tepper, D.; Magnes, B.-Z.; Pines, D.; Barak, T. *Ber. Bunsen−Ges. Phys. Chem.* **1998**, *102*, 504. (c) Pines, E.; Magnes, B.-Z.; Barak, T. *J. Phys. Chem. A* **2001**, *105*, 9674.
(35) Romsted, L. S. In *Surfactants in Solution*; Mittal, K. L., Lindman, B., Eds.; Plenum Press: New York, 1984; Vol. 2, p 1015.
(36) (a) Martinek, K.; Yatsimirski, A. K.; Levashov, A. V.; Berezin, I. V. In *Micellization, Solubilization and Microemulsions*; Mittal, K. L., Ed.; Plenum Press: New York−London, 1977; Vol. 2, p 489. (b) Romsted, L. S. In *Micellization, Solubilization and Microemulsions*; Mittal, K. L., Ed.; Plenum Press: New York−London, 1977; Vol. 2, p 509.
(37) (a) Kuzmin, M. G.; Soboleva, I. V. *J. Photochem Photobiol. A* **1995**, *87*, 43. (b) Soboleva, I. V.; Van Stam, J.; Dutt, G. B.; Kuzmin, M. G.; De Schryver, F. C. *Langmuir* **1999**, *15*, 6201. (c) Soboleva, I. V.; Kuzmin, M. G. *Russ. J. Phys. Chem*. **2000**, *74*, 1569.
(38) Pu, R. Y.; Wang, Y.; Ying, C.-H. *Biophys. Chem*. **1995**, *53*, 283.
(39) (a) Buu-Hoi, Ng. Ph.; Seallies, J. *J. Org. Chem*. **1955**, *20*, 606. (b) *Organic Reactions*; Adams, R., Ed.; Wiley: New York, 1942; Vol. 1, p 341.
(40) Knochenmuss, R.; Leutwyler, S. *J. Chem. Phys*. **1989**, *91*, 1268.
(41) Abuin, E.; Lissi, E. *J. Coll. Interface Sci.* **1986**, *112*, 178.
(42) Agmon, N.; Pines, E.; Huppert, D. *J. Chem. Phys.* **1988**, *88*, 5631.
(43) Weller, A. *Prog. React. Kinet.* **1961**, *1*, 187.
(44) Pines, E.; Pines, D.; Barak, T.; Magnes, B. Z.; Tolbert, L. M.; Haubrich, J. E. *Ber. Bunsen−Ges. Phys. Chem.* **1998**, *102*, 511.
(45) Tolbert, L. M.; Solntsev, K. M. *Acc. Chem. Res.* **2002**, *35*, 19 and references therein.
(46) Pina, F.; Melo, M. J.; Alves, S.; Ballardini, R.; Maestri, M.; Passaniti, P. *New J. Chem*. **2001**, *25*, 747.
(47) Solntsev, K. M.; Abou Al-Ainain, S.; Il'ichev, Yu. V.; Kuzmin, M. G., unpublished results.
(48) (a) Fernandez, M. S.; Fromherz, P. *J. Phys. Chem.* **1977**, *81*, 1755. (b) Hobson, R. A.; Grieser, F.; Healy, T. W. *J. Phys. Chem.* **1994**, *98*, 274.
(49) Marcus, R. A. *Faraday Discuss. Chem. Soc.* **1982**, *74*, 7.
(50) Zaitsev, N. K.; Demyashkevich, A. B.; Kuz'min, M. G. *Proc. Acad Sci. USSR, Chem. Sec.* **1980**, *255*, 622.
(51) Arnaut, L. G.; Formosinho, S. J. *J. Photochem. Photobiol., A* **1993**, *75*, 1.
(52) Marzzacco, C. J.; Deckey, G.; Colarulli, R.; Siuzdak, G.; Halpern, A. M. *J. Phys. Chem.* **1989**, *93*, 2935.
(53) (a) Moreira, P. F., Jr.; Giestas, L.; Yihwa, C.; Vautier-Giongo, C.; Quina, F. H.; Macanita, A. L.; Lima, J. C. *J. Phys. Chem. A* **2003**, *107*, 4203. (b) Vautier-Giongo, C.; Yihwa, C.; Moreira, P. F., Jr.; Lima, J. C.; Freitas, A. A.; Alves, M.; Quina, F. H.; Macanita, A. L. *Langmuir* **2002**, *18*, 10109. (c) Macanita, A. L.; Moreira, P. F., Jr.; Lima, J. C.; Quina, F. H.; Yihwa, C.; Vautier-Giongo, C. *J. Phys. Chem. A* **2002**, *106*, 1248.
(54) Politi, M. J.; Fendler, J. H. *J. Am. Chem. Soc.* **1984**, *106*, 265.
(55) (a) Harada, S.; Yano, H.; Yamashita, T.; Nishioka, S.; Yasunaga, T. *J. Coll. Interface Sci.* **1986**, *110*, 272. (b) Isoda, T.; Yamasaki, M.; Yano, H.; Sano, T.; Harada, S. *J. Chem. Soc., Faraday Trans.* **1994**, *90*, 869.
(56) Dumas, S.; Eloy, D.; Jardon, P. *New J. Chem.* **2000**, *24*, 711.
(57) (a) Gutman, M.; Nachliel, E.; Gershon, E.; Giniger, R *Eur. J. Biochem.* **1983**, *134*, 63. (b) Gutman, M.; Nachliel, E. *Biochemistry* **1985**, *24*, 2941.
(58) Agmon, N. *J. Phys. Chem*. **1996**, *100*, 1072.
(59) (a) Fisher, H.; DeCandis, F. X.; Ogden, S. D.; Jencks, W. P. *J. Am. Chem. Soc.* **1980**, *102*, 1340. (b) Yates, K. *J. Am. Chem. Soc.* **1986**, *108*, 6511. (c) Guthrie, J. P. *J. Am. Chem. Soc.* **1996**, *118*, 12886.
(60) Barzykin, A. V.; Shushin, A. I. *Biophys. J.* **2001**, *80*, 2062.
(61) (a) Šolc, K.; Stockmayer, W. H. *J. Chem. Phys.* **1971**, *54*, 2981. (b) Šolc, K.; Stockmayer, W. H. *Int. J. Chem. Kinet.* **1973**, *5*, 733. (c) Shoup, D.; Lipari, G.; Szabo, A. *Biophys. J.* **1981**, *36*, 697. (d) Berg, O. G. *Biophys. J.* **1985**, *47*, 1. (e) Schlosshauer, M.; Baker, D. *J. Phys. Chem. B* **2002**, *106*, 12079.
(62) Venables, D. S.; Schmuttenmaer, C. A. *J. Chem. Phys.* **1998**, *108*, 4935.
(63) Saeki, M.; Ishiuchi, S.-I.; Sakai, M.; Fujii, M. *J. Phys. Chem. A* **2001**, *105*, 10045.
(64) Il'ichev, Yu. V.; Solntsev, K. M.; Gridnev, I. D., unpublished results.